Lyra et al., J Clin Exp Oncol 2017, 6:2
DOI: 10.4172/2324-9110.1000180

Journal of Clinical & Experimental Oncology

Case Report

A SCITECHNOL JOURNAL

High Extra-Tumoral ^{99m}Tc-Macroaggregated Albumin Accumulation in a Fatty Liver in a Candidate for Transarterial Radioembolization Treatment

Vassiliki Lyra[1*], Konstantinos Palialexis[2], Chrisostomos Constantos[2], Lazaros Reppas[2], Elias N Brountzos[2] and Sofia N Chatziioannou[1]

Abstract

A patient with non-alcoholic fatty liver disease (NAFLD) and unresectable small-sized (≤3 cm) diffuse liver metastases from adenocarcinoma of the rectosigmoid junction was assessed for treatment with transarterial radioembolization (SIRT). The right hepatic arteriogram demonstrated several hypervascular lesions. However, the planar and the SPECT images of the subsequent right hepatic arterial ^{99m}Tc-MAA perfusion scintigraphy, revealed significantly heterogeneous distribution of ^{99m}Tc-MAA particles and "hot spots", not corresponding to lesion-specific sites.

The noncoincidence of the angiographic and the scintigraphic findings could be possibly influenced by hemodynamic changes, due to the presence of significant NAFLD. Because of the high risk-benefit ratio, the patient was considered to be an inappropriate candidate for SIRT.

Keywords

Transarterial radioembolization; SIRT; ^{90}Y-microspheres; ^{99m} Tc-MAA; Liver metastases; Liver tumor

Introduction

The local control of liver metastases represents the most reliable way to increase survival in metastatic ColoRectal Cancer (mCRC), since liver failure is responsible for the overwhelming majority of deaths, with surgery achieving the overall highest 5-year and 10-year survival for these patients [1]. Despite the latest expanded resectability criteria, based mainly on the future liver remnant [2], up to one fourth of patients with mCRC are diagnosed with liver metastases at presentation, the majority of which has unresectable disease [3,4]. The local control of unresectable disease by liver-directed ablation and embolization therapies, such as Selective Internal Radioembolization Treatment (SIRT) with ^{90}Y-SIR-Spheres, has already demonstrated a positive clinical impact, as a salvage therapy [5,6]. Recent published data have achieved promising results in improving progression free-survival and extending resectability, when used in combination with systemic new multi-drug (cytotoxic and biological agents) therapy [7,8]. Large sample randomized trials are ongoing; in order to better determine the patient benefit [9]. SIRT planning is based on hepatic arterial perfusion scintigraphy, which implicates the selective administration of ^{99m}Tc-Macro-Aggregated Albumin (^{99m}Tc-MAA) into the common hepatic artery or its branches, during the angiography procedure. The lung shunt fraction (LSF) [10,11] and the tumoral to non-tumoral ^{99m}Tc-MAA accumulation tissue ratio (TNR) [11-13] is assessed on the acquired planar and SPECT images. Patients with high LSF and/or low TNR should be excluded from radioembolization treatment, due to increased risk of radiation induced lung and/or hepatic injury [13,14].

We describe a case of SIRT planning assessment in a fatty liver with multiple small liver metastases from rectal cancer. An unexpectedly high ^{99m}Tc-MAA distribution in the non- tumoral liver tissue was achieved.

Case

A 73- year's old man, in a well-preserved performance status, a former smoker with a normal weight and no history of alcohol consumption, experienced the worsening of a long onset rectorrhagia. His medical history resulted a long-standing diagnosis of familiar hypertriglyceridemia and diabetes mellitus type 2. He had a surgical treatment for prostate and laryngeal cancer about six and four years ago, respectively, and since then he was free of disease. The endoscopic examination of the large bowel, performed to investigate the enterorrhagia revealed a high rectal mass. The specimen biopsy showed a moderately differentiated adenocarcinoma. Imaging procedures, such as fluorine-18-fluorodeoxyglucose positron emission tomography /computed tomography (^{18}F-FDG-PET/CT), demontrated a T3N0M1 rectal cancer with multiple small-sized (<3 cm) liver limited metastases (Figure 1). A low anterior resection of the primary rectal cancer was immediately undertaken, due to the rectal bleeding, and the low rectal tumor burden which required no extensive surgical excision. Five weeks following surgery, the patient received four cycles of XELOX and four cycles of FOLFOXIRI/Panitumumab, as first-line and second-line chemotherapy treatment, respectively. The multidrug therapy had no impact on the resectability conversion of the metastatic disease but at least, a stable disease was achieved.

At this point, the application of a liver-directed therapy was assessed as a salvage treatment. Due to the several, in various depths, small-sized liver lesions, radioembolization treatment with ^{90}Y-SIR-spheres was considered. However, patient had an increased hepatotoxic risk due to the presence of significant steatosis (Non-Alcoholic Fatty Liver Disease, NAFLD), revealed by the staging computed tomography scan (CT). As it is well known, the presence of a fatty-appearing liver on unenhanced CT scan (Figure 2), indicates a significant NAFLD and the most common pattern is the more or less irregular "diffuse" fat deposition, in accordance to the regional portal flow, with or without " All liver biochemistry tests were normal and thus, five months after the primary tumor resection, patient underwent a SIRT planning angiography procedure, during which the selective right (Figure 3) and left hepatic arteriogram clearly revealed the presence of neoangiogenetic lesions.

***Corresponding author:** Vassiliki Lyra, Department of Radiology, Nuclear Medicine Section, National and Kapodistrian University of Athens, Attikon Hospital, 1 Rimini St., Athens 12462, Greece, Tel: 00302107452045, 00306946361907; Fax: 00302105831778; E-mail: vslyra@yahoo.gr, vassilikilyra@gmail.com

Received: February 16, 2017 **Accepted:** February 28, 2017 **Published:** March 07, 2017

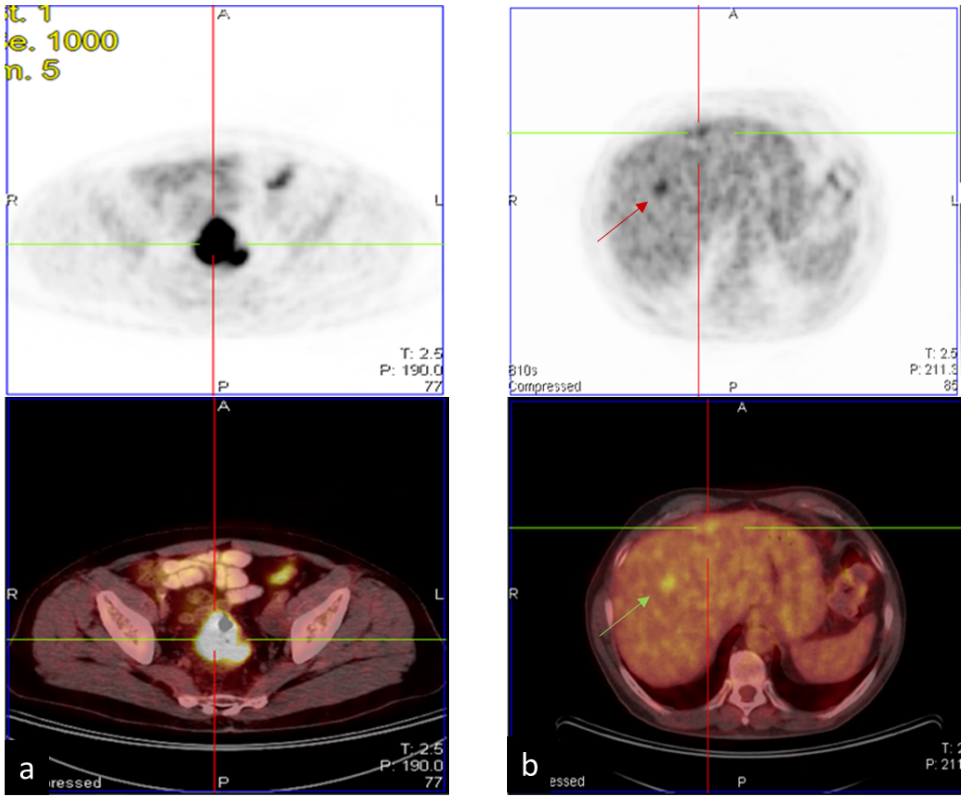

Figure 1: Patient's ^{18}F-FDG-PET/CT staging scan.

Note: Increased ^{18}F-FDG uptake by the primary rectal cancer (SUVmax=15) (intersection lines, figure 1a) and two of the small metastases of the right hepatic lobe, at the segment VIII (SUVmax=5.1) and the segment IVA (SUVmax=3.6) (arrow and intersection lines, figure 1b) are demonstrated.

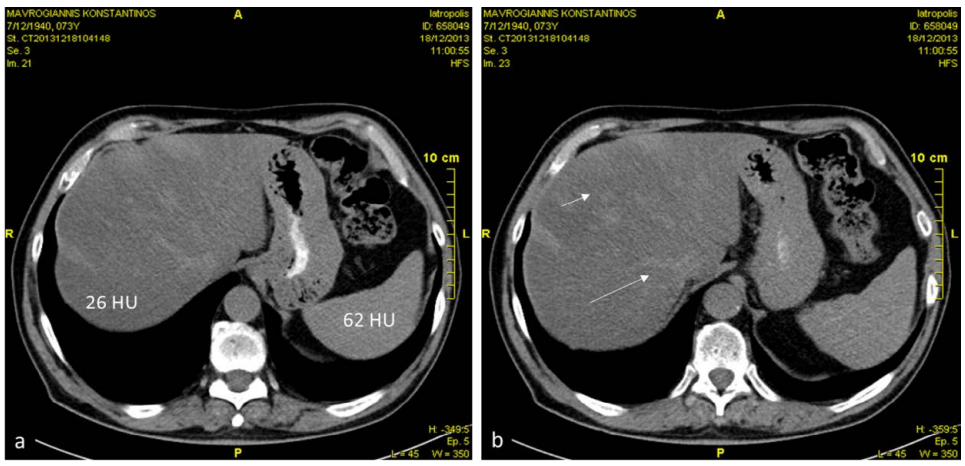

Figure 2: Patient's unenhanced CT staging scan.

Note: The attenuation criteria for the diagnosis of significant steatosis are largely satisfied (Figure 2a). Moreover, due to the significant low liver attenuation, the hepatic vasculature (arrow), and some of the metastases (arrowhead), appear hyperattenuated (Figure 2b).

The "staged" approach (distinct radioembolization treatment for each hepatic lobe within a 30-day interval) [5,11], was considered safer than the "whole" liver approach. Thus, after a prophylactic coil embolization of all visible extrahepatic vessels originating from the hepatic vasculature (Figure 3), 148MBq of ^{99m}Tc-MAA, approximately 200.000 particles of an average diameter of 35 μm (MAASOL, GE Healthcare), were administered by cathether position into the right hepatic artery. ^{99m}Tc-MAA scintigraphy data were acquired approximately half an hour after injection at the department of nuclear medicine, by a single-head GE Millenium gamma camera, with a LEHR collimator and an energy window set at 140keV ± 15%. No extrahepatic distribution of ^{99m}Tc-MAA was revealed on the whole-body planar images (Figure 4) and the calculated LSF was 2.2%. However, a significantly disomogeneous ^{99m}Tc-MAA distribution in

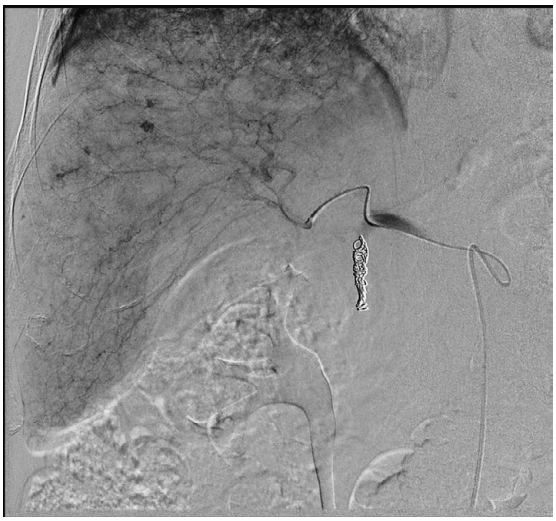

Figure 3: Patient's pre-SIRT liver angiography.

Note: The injection of contrast media by catheter into the right hepatic artery, demonstrates several small hypervascularized metastases with their tortuous neoangiogenetic vascular network (arrows). A prophylactic coil embolization of gastroduodenal artery is also noticed.

the right lobe, with elevated and faint activity areas and some "hot spots", mimicking the presence of underlying metastatic disease were most evident (Figure 4). Abdominal SPECT imaging (64 views of 20 sec each, stored in a 128×128 matrix, for a 360°orbit) confirmed the absence of ^{99m}Tc-MAA delivery outside the liver and its highly irregular distribution in the hepatic lobe parenchyma (Figure 5). Cross-sectional evaluation of SPECT with CT data did not reveal any specific radiotracer accumulation that could be attributed to the liver metastases.

Consequently, the unfavorable ratio between the predicted effectiveness of radioembolization treatment (responsiveness of metastatic disease) and the risk of Radioembolization Induced Liver Disease (REILD), leaded to the postponement of patient's ^{90}Y-SIR-Spheres administration for more suitable contingent.

Discussion

NAFLD is the most common cause of hepatic steatosis (20% of patients planned for hepatectomy) [17] and may be considered as the hepatic component of the metabolic syndrome [18]. Patient's fasting serum triglycerides were always elevated, even over 1000 mg/dl, although they were controlled much better in the past few years. Familiar hypertriglyceridemia (three of our patient's brothers also had hypertriglyceridemia), is a common autosomal dominant disorder, whose genetic and biochemical base is not yet understood. It often coexists with hyperglycemia, which acts aggravating to serum triglycerides levels [18].

Patients with NAFLD are considered more susceptible to chemotherapy-induced liver injury, and progression to Non-Alcoholic Steato-Hepatitis (NASH), due to the background of increased hepatocellular oxidative stress [19]. Moreover, fluorouracil, irinotecan and oxaliplatin which were included in the patient's chemotherapeutic regimen, have been specifically associated with increased risk of steatosis, steatohepatitis and sinusoidal obstruction syndrome, respectively [20,21].

The delivery of ^{99m}Tc-MAA particles to metastatic disease during the hepatic intra-arterial perfusion scintigraphy for SIRT planning, is considered in general, although with some limitations [22], comparable to that of ^{90}Y-SIR-spheres and predictive of lesion responsiveness to the internal radiation [10,23]. However, despite the comparable hemodynamic performance, the ^{99m}Tc-MAA particles (greater variability of size and, consequently, of a specific activity), usually exaggerate [23,24] the flow differences between liver metastases as well as between them and normal tissue, compared to SIRT-microspheres (relative stable size and amount of radioactivity per sphere). Moreover, the high number of ^{90}Y-SIR-spheres injected (100-200 times more) compared to that of ^{99m}Tc-MAA particles, present an embolizing effect during their slow intra-arterial somministration, which probably change the flow profile and delivers the latter portion of microspheres to relatively hypovascular tumors [24]. Additionally, it should be noticed that the less selective (main hepatic artery compared to segmental branches), the intra-arterial somministration of ^{90}Y-microspheres or ^{99m}Tc-MAA particles (e.g. in case of diffuse metastatic disease, as patient's case) is, the higher will be the inhomogeneity of particle distribution to tumoral and normal liver parenchyma will be. The microspheres enter predominantly into the larger vessels with higher blood flow due to their axial flow (wall exclusion effect) [24]. The asymmetric branching generates inhomogeneity, since the larger microspheres will preferentially follow the main vessel and be progressively separated from the smaller ones. Consequently, a faint inhomogeneous activity of the normal liver tissue in planar ^{99m}Tc-MAA scintigraphy is common, just as common is the occasionally appearance of "hot spots", due to the increased radiotracer accumulation in otherwise normal liver areas [24]. So, in case of the unavailability of a hybrid system, the acquisition of SPECT data and their comparative evaluation with morphological CT data, either by using or not using any fusion techniques, are useful to avoid misinterpretations [23,24], as in our patient's case. This "structured heterogeneity" of particles' delivery, which was recently confirmed at a microscopic level [25], is considered important for the "liver-sparing" effect on dose distribution [26].

Significant heamodynamics changes occur early in NASH, as it was recently demonstrated by xenon CT [27] and a contrast Ultrasonography Doppler scan [28]. The blood flow to the low resistance/low pressure portal vein system (Portal Vein Total Blood Flow, PVTBF), was less in NASH (even in simple steatosis) at an earlier stage, compared to chronic Hepatitis-C [27]. This is due to

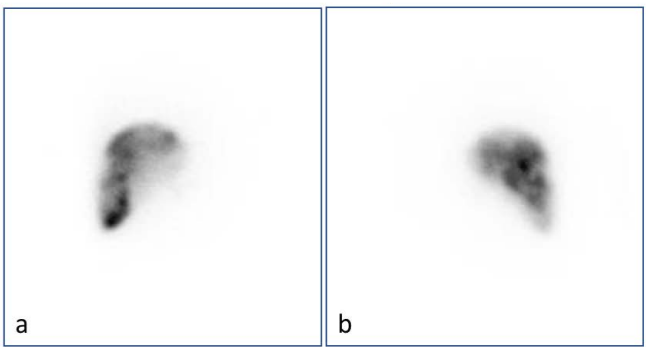

Figure 4: Patient's pre-SIRT liver perfusion imaging.

Note: A significant heterogeneous distribution of ^{99m}Tc-MAA is demonstrated on planar anterior (Figure 4a) and posterior images (Figure 4b) of the right hepatic lobe. There are "hot spots" not corresponding to metastases.

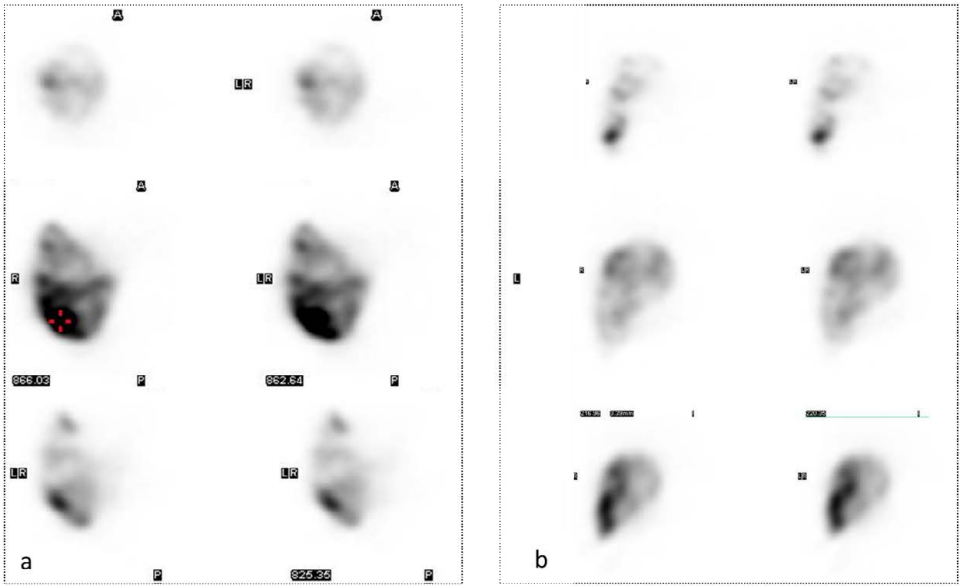

Figure 5: Patient's pre-SIRT liver perfusion imaging.

Note: The transaxial SPECT images from the upper to the lower areas (Figure 5a) and the coronal SPECT images from the anterior to the posterior areas (Figure 5b) of the right hepatic lobe, confirmed the mismatch between the ^{99m}Tc-MAA distribution and the lesions' localization.

the impairment of fatty liver microcirculation, which is not only correlated to the degree of perisinusoidal fibrosis but also to that of hepatocellular fat infiltration that compresses the sinusoidal networks [29]. On the other hand, (Hepatic Total Blood Flow, HTBF) is relatively maintained despite the steatosis and the fibrosis, by increasing HATBF (Hepatic Arterial Total Blood Flow), due to the compensatory mechanism of the "Hepatic Arterial Buffer Response", designed for HTBF preservation. HTBF is most important, not only for the metabolic needs of the liver but also for the homeostatic needs of the entire body [30].

It still remains unclear which individuals with moderate to severe NAFLD, are at greater risk for progression (10-20% of cases) to inflammatory NASH, although it is probable that the more severe the steatosis and the risk factors are, like diabetes, the more likely it becomes to be complicated by steatohepatitis (NASH) [31]. The available imaging techniques cannot differentiate steatohepatitis from steatosis, since they are unreliable in diagnosing mild degrees of fibrosis [29]. There is also a poor correlation between biochemical and histological findings (silent NASH), since all spectrums of the histological NASH findings were found in patients with normal liver biochemistry [31].

In summary, the patient's imaging was conformed to multiple small metastases of <3 cm and a severe fatty infiltration of the liver. Only, a liver biopsy, which was not performed, could have had address the compresence of steatohepatitis and the genomic characteristics (e.g. K-RAS status) of liver metastases as well. The subsequent hepatic arteriogram did not reveal any liver vascularization problems and brought out multiple small hypervascularized lesions. Conversely, the ^{99m}Tc-MAA-intra-arterial scintigraphy demonstrated a significant heterogeneous irrigation into the different segments without any apparent accumulation at the lesions. According to previous considerations, the heterogeneous distribution of ^{99m}Tc-MAA particles could possibly be enchanced by the underlying HATBF changes, characterizing NAFLD or NASH. It should be noticed that the majority of patient's small-sized lesions were not affected by limit resolution and partial volume effect of SPECT imaging, and they would be clearly distinguishable in case of a more favourable distribution of the background activity. Moreover, despite some data in apparent conflict about the tumor size and the TNR [12], the most pronounced arterialization is actually found in the rim of metastases >1.5 cm, followed by that of metastases <1.5 cm, and finally by the central area of larger metastases [25]. So, the patient's blood flow in preferential arterial hepatic ways resulted in marked radiotracer activity differences through hepatic parenchyma and prevented the emergence of the small-sized metastases and that of a favourable TNR (tumoral to non-tumoral tissue ratio).

At this point, the patient SIRT planning re-assessment, following the intra-arterial administration of angiotensin II (ATII) was evaluated, in order to re-distribute arterial blood flow from non-tumoral to tumoral areas. Recently available data [32] demonstrated a significant improvement of the arterial blood supply of liver metastases using ATII (up to ten times for the smaller ones, using intra-operative Doppler flowmetry), due to the lack of its vasoconstrictor effect on immature tumor vessels. However, the uncertainty of the baseline perfusion, even for the larger lesions, discouraged a new attempt of SIRT planning assessment under pharmacological intervention.

Conclusion

During SIRT planning for diffuse small-sized metastatic disease therapy, the background of severe NAFLD could address a low TNR and a highly heterogeneous distribution of ^{99m}Tc-MAA particles, due to microcirculation flow modifications. These findings increase the risk of REILD obviating radioembolization treatment with ^{90}Y-microspheres.

References

1. Tomlinson JS, Jarnagin WR, DeMatteo RP, Fong Y, Kornprat P, et al. (2007) Actual 10-year survival after resection of colorectal liver metastases defines cure. J Clin Oncol 25: 4575-4580.

2. Pawlik TM, Schulick RD, Choti MA (2008) Expanding criteria for resectability of colorectal liver metastases. The Oncologist 13: 51-64.

3. Siriwardena AK, Mason JM, Mullamitha S, Hancock HC, Jegatheeswaran S (2014) Management of colorectal cancer presenting with synchronous liver metastases. Nat Rev Clin Oncol 11: 446-459.

4. Macedo FI, Makarawo T (2014) Colorectal hepatic metastases: Evolving therapies. World J Hepatol 6: 453-463.

5. Rosenbaum CE, Verkooijen HM, Lam MG, Smits ML, Koopman M, et al. (2013) Radioembolization for treatment of salvage patients with colorectal cancer liver metastases: a systematic review. J Nucl Med 54: 1890-1895.

6. Saxena A, Meteling B, Kapoor J, Golani S, Morris DL, et al. (2015) Is Yttrium-90 radioembolization a viable treatment option for unresectable, chemorefractory colorectal cancer liver metastases? A large single-center experience of 302 patients. Ann Surg Oncol 22: 794-802.

7. Kennedy AS, Ball D, Cohen SJ, Cohn M, Coldwell DM, et al. (2015) Multicenter evaluation of the safety and efficacy of radioembolization in patients with unresectable colorectal liver metastases selected as candidates for ^{90}Y resin microspheres. J Gastrointest Oncol 6: 134-142.

8. Braat AJ, Huijbregts JE, Molenaar IQ, Borel Rinkes IH, van den Bosch MA, et al. (2014) Hepatic radioembolization as a bridge to liver surgery. Front Oncol 4: 199.

9. Van Hazel GA, Heinemann V, Sharma NK, Findlay M, Ricke J, et al. (2016) SIRFLOX: Randomized phase III trial comparing first-line mFOLFOX6 (plus or minus bevacizumab) versus mFOLFOX6 (plus or minus bevacizumab) plus selective internal radiation therapy in patients with metastatic colorectal cancer. J Clin Oncol 34: 1723-1731.

10. Lenoir L, Edeline J, Rolland Y, Pracht M, Raoul JL, et al. (2012) Usefulness and pitfalls of MAA SPECT/CT in identifying digestive extrahepatic uptake when planning liver radioembolization. Eur J Nucl Med Mol Imaging 39: 872-880.

11. Giammarile F, Bodei L, Chiesa C, Flux G, Forrer F, et al. (2011) EANM procedure guidelines for the treatment of liver cancer and liver metastases with intra-arterial radioactive compounds. Eur J Nucl Med Mol Imaging 38: 1393-1406.

12. Lambert B, Mertens J, Sturm EJ, Sticnaers S, Defreyne L, et al. (2010) ^{99m}Tc-labelled MAA scintigraphy for planning treatment with ^{90}Y-microspheres. Eur J Nucl Med Mol Imaging 37: 2328-2333.

13. Cremonesi M, Chiesa C, Strigari L, Ferrari M, Botta F, et al. (2014) Radioembolization of hepatic lesions from a radiobiology and dosimetric perspective. Frontiers in Oncology 4:210.

14. Riaz A, Awais R, Salem R (2014) Side effects of yttrium-90 radioembolization. Front Oncol 4:198.

15. Hamer OW, Aguirre DA, Casola G, Lavine JE, Woenckhaus M, et al. (2006) Fatty liver: Imaging patterns and pitfalls. Radiographics 26: 1637-1653.

16. Décarie PO, Lepanto L, Billiard JS, Olivié D, Murphy-Lavallée J, et al. (2011) Fatty liver deposition and sparing: a pictorial review. Insights Imaging 2: 533-538.

17. Abele JT, Fung CI (2010) Effect of hepatic steatosis on liver FDG uptake measured in mean standard uptake values. Radiology 254: 917-924

18. Straub BK, Schirmacher P (2010) Pathology and biopsy assessment of non-alcoholic fatty liver disease. Dig Dis 28: 197-202.

19. Hübscher SG (2006) Histological assessment of non-alcoholic fatty liver disease. Histopathology 49: 450-465.

20. Vauthey JN, Pawlik TM, Ribero D, Wu TT, Zorzi D, et al. (2006) Chemotherapy regimen predicts steatohepatitis and an increase in 90-day mortality after surgery for hepatic colorectal metastases. J Clin Oncol 24: 2065-2072.

21. Robinson SM, Wilson CH, Burt AD, Manas DM, White SA (2012) Chemotherapy-associated liver injury in patients with colorectal liver metastases: a systematic review and mate-analysis. Ann Surg Oncol 19: 4287-4299.

22. Wondergem M, Smits M, Elschot M, de Jong H, Verkooijen HM, et al. (2013) ^{99m}Tc- MAA poorly predicts the intrahepatic distribution of ^{90}Y Resin microspheres in hepatic radioembolization. J Nucl Med 54: 1294-1301.

23. Ulrich G, Dudeck O, Furth C, Ruf J, Grosser O, et al. (2013) Predictive value of intratumoral ^{99m}Tc- Macroaggregated uptake in patients with colorectal liver metastases scheduled for radioembolization with ^{90}Y-microspheres. J Nucl Med 54: 516-522.

24. Van de Wiele C, Maes A, Brugman E, D'Asseler Y, De Spiegeleer B, et al. (2012) SIRT of liver metastases: physiological and pathophysiological considerations. Eur J Nucl Med Mol Imaging 39: 1646-1655.

25. Högberg J, Rizell M, Hultborn R, Svensson J, Henrikson O, et al. (2014) Heterogeneity of microsphere distribution in resected liver and tumour tissue following selective intrahepatic radiotherapy. EJNMMI Res 4:48.

26. Spreafico C, Maccauro M, Mazzaferro V, Chiesa C (2014) The dosimetric importance of the number of ^{90}Y microspheres in liver transarterial radioembolization (TARE). EJNMMI 41: 634-638.

27. Shigefuku R, Takahashi H, Kato M, Yoshida Y, Suetani K, et al. (2014) Evaluation of hepatic tissue blood flow using xenon CT with fibrosis progression in NAFLD: comparison with chronic hepatitis C. Int J Mol Sci 15: 1026-1039.

28. Hirooka M, Koizumi Y, Miyake T, Ochi H, Tokumoto Y, et al. (2015) Nonalcoholic fatty liver disease: portal hypertension due to outflow block in patients without cirrhosis. Radiology 274: 597-604.

29. Farrell G, Teoh NC, McCuskey RS (2008) Hepatic microcirculation in fatty liver disease. The Anatomical Record 291: 684-692.

30. Schmidt R (2010) Regulation of hepatic blood flow: the hepatic arterial buffer response revisited World J Gastroenterol 16: 6046-6057.

31. Pedossa P (2016) Histological assessment of NAFLD. Dig Dis Sci 61: 1348-1355.

32. Van den Hoven AF, Smits ML, Rosenbaum CE, Verkooijen HM, van den Bosch MA, et al. (2014) The effect of intra-arterial angiotensin II on the hepatic tumor to non-tumor blood flow ratio for radioembolization: a systematic review. PLOSone 9: e86394.

Author Affiliations

Top

[1]*Department of Radiology, Nuclear Medicine Section, National and Kapodistrian University of Athens, Attikon Hospital, 1 Rimini St., Athens 12462, Greece*

[2]*Department of Radiology, Interventional Radiology Unit,National and Kapodistrian University of Athens, Attikon Hospital, 1 Rimini St., Athens 12462, Greece*